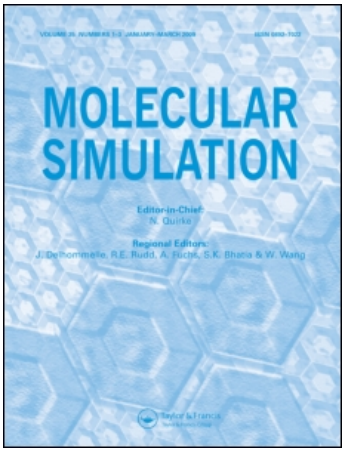

Molecular Simulation
Publication details, including instructions for authors and subscription information:
http://www.informaworld.com/smpp/title~content=t713644482

Nanoindentation as a Probe of Nanoscale Residual Stresses: Atomistic Simulation Results

O. Shenderova[a]; J. Mewkill[a]; D. W. Brenner[a]
[a] Department of Materials Science and Engineering, North Carolina State University, Raleigh, NC

To cite this Article Shenderova, O. , Mewkill, J. and Brenner, D. W.(2000) 'Nanoindentation as a Probe of Nanoscale Residual Stresses: Atomistic Simulation Results', Molecular Simulation, 25: 1, 81 — 91
To link to this Article: DOI: 10.1080/08927020008044114
URL: http://dx.doi.org/10.1080/08927020008044114

Molecular Simulation, 2000, Vol. 25, pp. 81–91
Reprints available directly from the publisher
Photocopying permitted by license only

NANOINDENTATION AS A PROBE OF NANOSCALE RESIDUAL STRESSES: ATOMISTIC SIMULATION RESULTS

O. SHENDEROVA*, J. MEWKILL and D. W. BRENNER

Department of Materials Science and Engineering,
North Carolina State University, Raleigh, NC 27695-7907

(Received April 1999; accepted May 1999)

Results from two sets of molecular dynamics simulations are reported. In the first set of simulations a nanoscale tip was used to indent single-crystal gold lattices subjected to external strains. These were carried out to explore possible relationships between nanoindentation curves and elastic properties of uniformly strained films. The changes in the slope of the loading curves reflect the stress state of the sample. In the second set of simulations the use of shallow nanoindentation for mapping nonuniform residual surface stress near a dislocation intersecting a surface was tested. Correlation between the maximum force on the tip and the initial local stresses at the point of indentation were observed. Preliminary atomistic simulations indicate that atomic-force microscopy can be used as a nondestructive, nanoscale probe of the surface stress distributions.

Keywords: Nanoindentation; residual stresses; gold; simulation

INTRODUCTION

Many applications of thin films and coatings require knowledge of their mechanical properties. Because of their small volumes, the mechanical properties of thin films may be significantly different from those in the bulk materials. One powerful method for measuring thin film mechanical properties is nanoindentation [1–5]. From analysis of indentation load-displacement data, it is possible in principle to obtain both local elastic moduli and hardnesses of thin films. However, real films often possess

*Corresponding author.

residual stresses, and it is well established experimentally that load-displacement curves measured by nanoindentation can be altered by stresses in the sample [1 – 5]. Tsui, Oliver and Pharr, for example, studied the influence of applied stress on the nanoindentation of an aluminum alloy [3]. They observed an increase in slope of the unloading curve with compressive stress, and a decrease in slope with tensile stress. This is consistent with previous studies on aluminum films [1, 2] and more recent studies of strained gold samples [5].

From an analysis of unloading curves, which assumes no change in contact area between the indentor and sample, it appears that the hardness and elastic modulus of stressed samples increases with compressive stress and decreases with tensile stress. This is consistent with the properties of bulk materials, where anharmonicities in the interatomic forces generally result in an increase in modulus under compression and a decrease under tension. For most FCC metals, for example, the Young's modulus decreases for tensile strain along the ⟨111⟩ and ⟨110⟩ directions (although the modulus increases for tensile strain along the ⟨100⟩ direction) [6 – 9]. The Young's modulus dependence on ⟨111⟩ uniaxial strain in gold calculated from phenomenological data Ref. [7] is illustrated in Figure 1. On the other hand, Tsui, Oliver and Pharr [3] argue that the magnitude of the changes in modulus and hardness for their samples obtained from standard analysis of the loading curves is too large to be accounted for by observable changes in material properties. Instead, they suggest that pile-up of

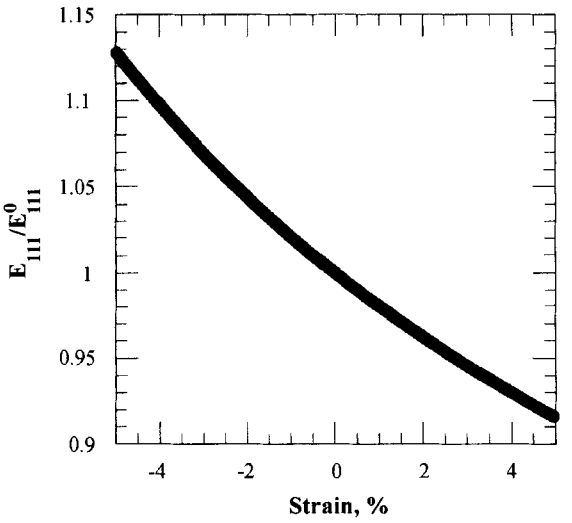

FIGURE 1 The Young's modulus dependence on ⟨111⟩ uniaxial strain in gold.

material surrounding the indentor causes a change in contact area that results in the changes in the slope of the indentation curves. This pileup is apparently promoted by compressive stress and diminished by tensile stress, leading to the observed changes in indentation data. This conclusion has been supported by finite element simulations [4].

Because the stress state of a film influences nanoindentation load-displacement curves, appropriate analysis of shallow indentation curves measured at different contact points could in principle be used to map local residual surface stress distributions. This would be extremely useful for characterizing the influence of surface features such as dislocations and steps on residual surface stresses [10, 11]. Such an analysis, however, would require a detailed understanding of the relationship between these stresses and the indentation data. A powerful tool to understand this relationship is atomistic modeling which gives us a way to calculate local atomic stresses in the indentation point prior and during the indentation.

In this paper, results from a series of molecular dynamics simulations are reported in which single-crystal gold samples subjected to external strains were indented (Fig. 2). These were carried out to explore possible relationships between nanoindentation curves and elastic properties of strained films. It is demonstrated that the effective modulus of the material, as

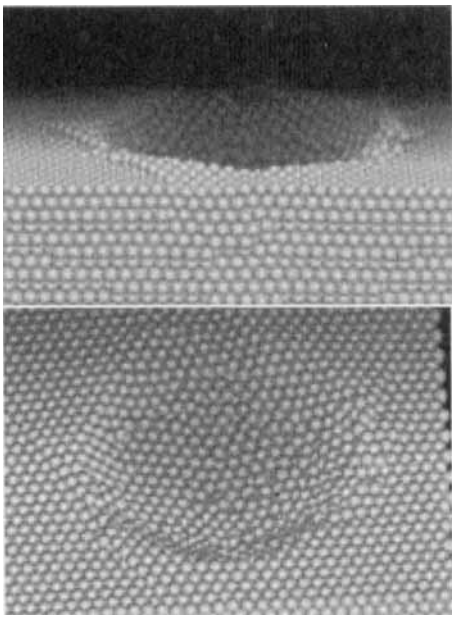

FIGURE 2 Snapshots from the simulated indentation of a single-crystal gold (111) surface.

determined from changes in the slope of the loading curves, increase under compression and decrease under tension. This is consistent with the experimental observations discussed above. Furthermore, the simulations demonstrate that for these relatively shallow indentation depths the true contact area is essentially independent of applied strain. Therefore we conclude that the changes in the slope of the load-displacement curves of strained films, at least for shallow indentation, may be connected with the true stress dependence of the elastic modulus of the sample. At a deeper indentation depth (more than approximately 10 Å) a raised lip of atoms surrounding the indentor was observed, which is a precursor to pile-up. The detailed analysis of atomic stress distribution in the vicinity of an indentor, including the atoms that constitute the raised lip, revealed that atomic stresses in the lip are roughly half those in the bulk substrate. This suggests that the contribution of the material in the lip region to the resulting force acting on the tip is significantly lower than that from the rest of the substrate and this fact might be taken into account when analyzing the experimental data on nanoindentation in the presence of pile-up. To test the use of shallow nanoindentation for mapping residual surface stresses, simulated indentations were carried out on gold sample containing a dislocation intersecting the surface. Observed correlations between the maximum load for a constant indentation depth of 2.5 Å and residual surface stresses at the contact points support the potential use of shallow nanoindentation for mapping residual surface stress distributions.

METHOD OF CALCULATION

The simulations of a strained gold lattice used a system containing 24,576 atoms in an FCC lattice with a thickness 5.4 nm, periodic lateral dimensions of 9.2 nm by 8.0 nm, and a (111) surface orientation. The tip of a nanoindentor was modeled by a single sphere with radius 3.2 nm. Interatomic forces between atoms in the substrate were calculated using the embedded-atom method [12].

The tip-surface interaction was modeled with the repulsive region of a Lennard-Jones potential. This model excludes strong tip-substrate adhesive interactions, and is intended to model a surface with a passivating layer. The system was strained by scaling the in-plane atomic positions and periodic boundary conditions followed by relaxation of the system to the minimum energy configuration. The thickness of the strained substrate changed during the relaxation, yielding a Poisson ratio of $\nu_{yz} = 0.2$, for the given

lattice orientation. Indentation of the relaxed systems was simulated by numerically integrating classical equations of motion for the gold atoms using a constant timestep of 1 fs while moving the tip at a constant rate of 10^{-4} nm per timestep into the surface. In addition, hydrostatic and average shear atomic level stresses, attributed to the individual atoms [13], were calculated and plotted at the maximum indentation point. Loading curves were obtained by summing the forces on the tip at a given indentation depth. Maximum indentation depths of 7.5 Å and 17 Å were modeled; these correspond to the absence or presence of the raised lip of the surface, respectively. At both indentation depths the structure of the region beneath the indentor contained amorphous-like material within several atomic planes in the vicinity of the indentation point; the nucleation of dislocation loops was not observed. As discussed by Belak *et al.* [14], system size influences possible mechanisms the release of stored elastic energy during indentation. These can be either dislocation or non-dislocation mechanisms, where the latter tends to occur in smaller systems.

The second set of simulations modeled shallow indentation of a (112) surface of a single-crystal gold sample intersected by edge dislocations with Burgers vectors $\mathbf{b} = a/2\ \langle 110 \rangle$ lying along the $\langle 112 \rangle$ direction. A dislocation dipole, rather than a single dislocation, was required to maintain two-dimensional periodic boundary conditions. During energy minimization, the complete edge dislocations dissociated into two partials dislocations separated by a distance of approximately 6**b**. Indentation to a depth of 2 Å was repeated for 40 points around one of the dislocation cores.

RESULTS

The load-displacement curves up to an indentation depth of 7.5 Å relative to the top surface layer for the strained and unstrained substrates are plotted in Figure 3. Raising of surface atoms around the indentor was not observed for any of these cases. The highest strains studied, 7% (both compression and tension), are significantly higher than the experimental efforts [5]. These were used in this simulation to enhance the differences in the strained system behavior originating from the anharmonicity of the inter-atomic interactions. The effective elastic modulus of a tip-substrate system can be calculated using the expression [15]:

$$dF/dh = 2(AE^*/\pi)^{1/2} \tag{1}$$

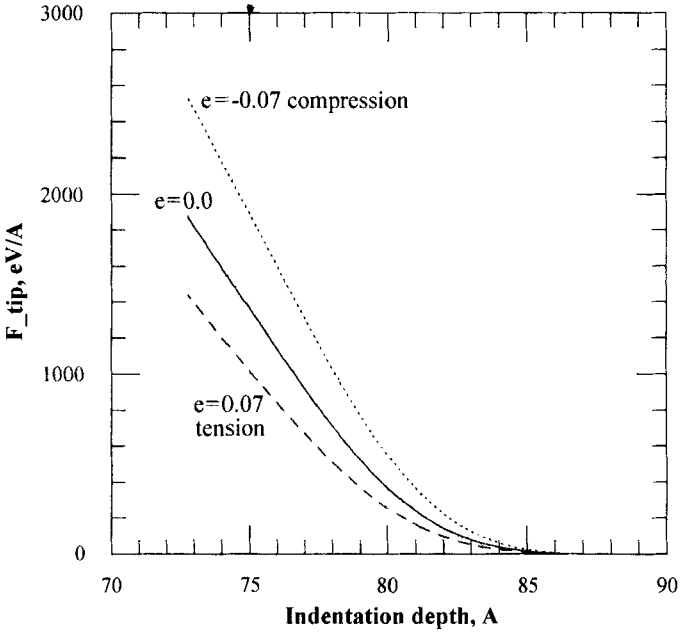

FIGURE 3 Load-displacement curves for different deformation states of the sample.

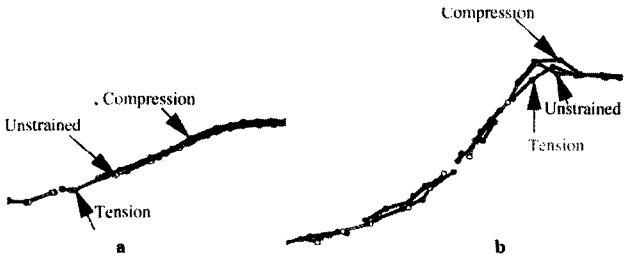

FIGURE 4 Cross sections of the indentation profiles of the strained substrates in the absence (a) and presence (b) of a pileup.

where F is the force applied on the tip, h is tip displacement, A is the contact area, and E^* is the modulus. This expression, which was derived by Pharr and coworkers [15] based on the analysis of Sneddon [16], is valid for any tip having the shape of a solid of revolution. Cross sections of one-half of the indentation surface profiles of the strained and unstrained substrates are illustrated in the Figure 4a, where atoms of the first surface layer are illustrated. Apparently the indentation profile is essentially the same for all deformation states. Therefore any change in slope of the

loading curves can be attributed to changes in elastic modulus. Equation (1) together with the slopes of the loading curves in Figure 3 yield effective elastic modulii for the system under 7% compression and tension that are 13% higher and 11% lower, respectively, than the unstrained substrate. Thus, the influence of the compressive strain on the elastic modulus is higher in comparison with that of the tension due to anharmonicity of the interatomic interactions. It can be concluded that at these shallow indentation depths, the contact area is strain independent in the absence of a pile up and observed changes in the slopes of the indentation curves in the strained substrates are connected with the strain dependence of the elastic modulus. At very shallow indentation depth the relative sensitivity of the tip to changes in the strained sample become more pronounced [17]. The change in force on the tip relative to applied strain appeared to be more pronounced at indentation depths of approximately two atomic layers. This is connected with the specific stress state of atoms near the surface due to surface relaxation.

At a deeper indentation depth of 17 Å, gold atoms at the surface-tip interface were raised above the surrounding surface (Fig. 4b). The raised lip of atoms was promoted by external compressive strains and diminished by external tensile strains relative to the unstrained sample; this is consistent with finite-element simulations that predict pile-up. The height of the lip above the sample surface was 1.4 Å, 1.7 Å and 2.2 Å for the substrate at maximum tension, unstrained, and under maximum compression, respectively. Although the raised lip changes the actual contact area (similar to pile-up characterized by finite element studies), atomic stresses of the atoms that constitute the lip are roughly half those in the bulk substrate (Fig. 5). Thus the contribution of the material in the raised lip region to the resulting force acting on the tip is significantly lower than that from the

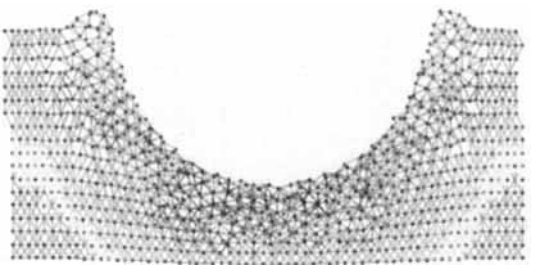

FIGURE 5 Illustration of the distribution of average shear stresses at maximum indentation depth. (See Color Plate I).

rest of the substrate. Average shear stresses for atoms in each of these regions are illustrated in Figure 5. Darker colors correspond to higher stress values. Stress scale corresponds to that in Figure 6.

The stress distributions calculated from the interatomic potential can be used to further characterize features of the indentation; these can also be compared to predictions from continuum mechanics. For each strain state, shear stresses in the indented substrate were concentrated along the three (111) slip planes surrounding the contact point, and reached a maximum value in the sample below the indentor. When the sample was biaxially stretched, the shear stresses increased in magnitude and in extension beneath the indentor (Fig. 6). Biaxial compression, in contrast, diminished the shear stresses beneath the indentor (Fig. 6). Uniaxial tension resulted in the same trends in shear stress as was observed for biaxial tension. For uniaxial compression, however, the shear stresses were unaffected. Thus the influence of compression on the magnitudes and distribution of shear stresses differs between uniaxial and biaxial loading. These observations are consistent with the conclusions of continuum mechanics [3, 18].

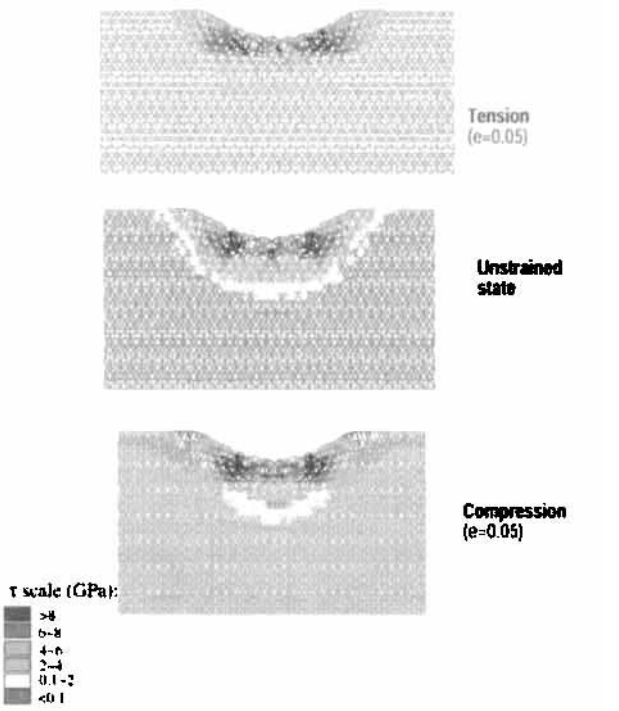

FIGURE 6 Atomic average shear stress profile near the indentation point at biaxial strain. (See Color Plate II).

strictly in-plane residual stresses. These results support the use of nanoscale indentation for mapping residual surface stress distributions.

CONCLUSION

Molecular dynamics simulations of indentation of a single-crystal gold surface demonstrate that for relatively shallow indentation depths the true contact area is essentially independent of applied strain. Therefore it can be concluded that the changes in slopes of load-displacement curves of strained films, at least for shallow indentation, may be connected with the true stress dependence of the effective elastic modulus of the sample and tip. In cases where a raised lip was observed, stress within the region of the lip was found to be much less than that in the region of the sample below the indentor. This results in essentially lower contribution of atoms of the lip to the total force on the tip. Furthermore, nanoindentation results at very shallow depths show an increased sensitivity to changes in applied strain. The use of Atomic Force Microscopy to probe the surface of a sample for changes in local surface strains should be performed at very shallow indents to increase sensitivity and reduce pile-up.

Nanoindentation was also studied as a method to map the stresses surrounding surface features using as a model system dislocations intersecting a surface. Correlations between the maximum force on the tip and the initial local stresses in the point of indentation were observed, indicating that atomic-force microscopy can be used as a nondestructive, nanoscale probe of the surface stress distributions.

Acknowledgments

The EAM calculations were carried using a modified version of DYNAMO obtained from Sandia National Laboratory. We are grateful for helpful discussions with R. Colton, S. A. Syed Asif, K. F. Jarausch, P. J. Russell and J. Belak. This work was supported by the National Science Foundation through contract DMR-9502586.

References

[1] LaFontaine, W. R., Paszkiet, C. A., Korhonen, M. A. and Che-Yu Li (1991). *J. Mater. Res.*, **6**, 2084.
[2] LaFontaine, W. R., Yost, B. and Che-Yu Li (1990). *J. Mater. Res.*, **5**, 776.
[3] Tsui, T. Y., Oliver, W. C. and Pharr, G. M. (1996). *J. Mater. Res.*, **11**, 752.

[4] Bolshakov, A., Oliver, W. C. and Pharr, G. M. (1996). *J. Mater. Res.*, **11**, 760.
[5] Jarausch, K. F., Houston, J. E. and Russell, P. J., unpublished.
[6] Riley, M. W. and Skove, M. J. (1973). *Phys. Rev. B*, **8**, 466.
[7] Milstein, F. and Rasky, D. (1982). *Phil. Mag. A*, **45**, 49.
[8] Wolf, D. and Lutsko, J. F. (1989). *J. Mater. Res.*, **4**, 1427.
[9] Adams, J. B., Wolfer, W. G. and Foiles, S. M. (1989). *Phys. Rev. B*, **40**, 9479.
[10] Shenderova, O. A., Mewkill, J., Linehan, P., Brenner, D., Jarausch, K. and Russell, P. (1998). *MRS Symp. Proc.*, **522**.
[11] Brenner, D. W., Schall, J. D., Mewkill, J. P., Shenderova, O. A. and Sinnott, S. B. (1998). *J. Brit. Inter. Soc.*, **51**, 137.
[12] Foils, S. M., Baskes, M. I. and Daw, M. S. (1986). *Phys. Rev. B*, **33**, 7983.
[13] Vitek, V. and Egami, T. (1987). *Phys. Stat. Sol. (b)*, **144**, 145.
[14] Belak, J., Glosli, J. N., Boerker, D. B. and Stowes, I. F. (1995). *MRS Symp. Proc.*, **389**, 181.
[15] Pharr, G. M., Oliver, W. C. and Brotzen, F. R. (1992). *J. Mater. Res.*, **7**, 613.
[16] Sneddon, I. N. (1965). *Int. J. Eng. Sci.*, **3**.
[17] Mewkill, J. P., unpublished.
[18] Meyers, M. A. and Chawla, K. K. (1984). *Mechanical Metallurgy: Principles and Applications*, Prentice-Hall.